

Measurements of jet quenching with semi-inclusive charged jet distributions in Au+Au collisions at $\sqrt{s_{NN}}=200$ GeV

P. M. Jacobs and A. Schmah for the STAR Collaboration*

Lawrence Berkeley National Laboratory, Berkeley CA, USA

Abstract

We report measurements of jet quenching in Au+Au collisions at $\sqrt{s_{NN}}=200$ GeV, based on the semi-inclusive distribution of reconstructed charged particle jets recoiling from a high p_T hadron trigger. Jets are reconstructed with the anti- k_T algorithm ($R=0.2$ to 0.5), with low IR-cutoff of track constituents ($p_T > 0.2$ GeV/ c). Uncorrelated background is corrected using a novel mixed-event technique, with no fragmentation bias imposed by the correction procedure on the accepted recoil jet population. Corrected recoil jet distributions, reported in the range $0 < p_{T,jet}^{ch} < 30$ GeV/ c , are used to measure jet yield suppression, jet energy loss, and intra-jet broadening. The first search for QCD Molière scattering of jets in hot QCD matter at RHIC is reported.

Keywords:

QCD, Jet Quenching, Quark-Gluon Plasma

The interaction of energetic jets with hot QCD matter (“jet quenching”) provides unique probes of the Quark-Gluon Plasma (QGP) generated in high energy collisions of heavy nuclei. Comprehensive understanding of jet quenching requires measurements of reconstructed jets and their correlations. Measurement of reconstructed jets in the high-multiplicity environment of heavy ion collisions is challenging, however, because of the large and inhomogeneous backgrounds in such events. In this proceedings the STAR Collaboration at RHIC reports measurements of jet quenching in central and peripheral Au+Au collisions at $\sqrt{s_{NN}}=200$ GeV, using an observable designed to address this challenge: the semi-inclusive distribution of reconstructed charged particle jets recoiling from a high p_T trigger hadron. A similar measurement has been carried out by the ALICE Collaboration at the LHC, for Pb+Pb collisions at $\sqrt{s_{NN}}=2.76$ TeV [1].

The data were recorded by STAR during the 2011 RHIC run with Au+Au collisions at $\sqrt{s_{NN}}=200$ GeV, using a minimum bias trigger. Offline analysis is carried out using charged tracks measured by the STAR Time Projection Chamber (TPC). Events are classified in percentile intervals of uncorrected multiplicity of charged tracks within $|\eta| < 0.5$; this analysis uses events in the 0–10% (“central”) and 60%–80% (“peripheral”) percentile intervals. One trigger hadron per event is selected randomly from all observed charged particles with $p_T > 9$ GeV/ c . Charged jets, composed of charged tracks, are reconstructed using the anti- k_T algorithm [2] with the boost-invariant p_T -recombination scheme, for resolution parameter $R = 0.2, 0.3$,

*pmjacobs@lbl.gov, aschmah@lbl.gov

0.4 and 0.5. The raw reconstructed jet energy for each jet candidate i , $p_{T,jet}^{raw,i}$, is shifted by the estimated background energy in the jet area,

$$p_{T,jet}^{reco,i} = p_{T,jet}^{raw,i} - \rho \cdot A_{jet}^i, \quad (1)$$

where ρ is the estimated median background energy density in the event, and A_i is the jet area. Jet acceptance is $|\eta_{jet}| < 1.0 - R$, based on the jet centroid. A jet area cut suppresses background jets while preserving high efficiency for true hard jets. Since ρ is the median background level in the event, $p_{T,jet}^{reco,i}$ can be negative; we expect that region to be dominated by background that is uncorrelated to the trigger.

The semi-inclusive recoil jet distribution is equivalent to the ratio of inclusive production cross sections,

$$\frac{1}{N_{trig}^{AA}} \cdot \frac{d^2 N_{jet}^{AA}}{dp_{T,jet}^{ch} d\Delta\varphi} = \left(\frac{1}{\sigma^{AA \rightarrow h+X}} \cdot \frac{d^2 \sigma^{AA \rightarrow h+jet+X}}{dp_{T,jet}^{ch} d\Delta\varphi} \right), \quad (2)$$

where AA denotes pp or Au+Au collisions; $\Delta\varphi = |\varphi_{trig} - \varphi_{jet}|$; $\sigma^{AA \rightarrow h+X}$ is the inclusive cross section to generate a trigger hadron; and $d^2 \sigma^{AA \rightarrow h+jet+X} / dp_{T,jet}^{ch} d\Delta\varphi$ is the inclusive differential cross section for coincidence production of a trigger hadron and recoil jet. The recoil acceptance is $|\pi - \Delta\varphi| < \pi/4$. After correction for uncorrelated background, the distribution in Eq. 2 is the absolutely normalized recoil jet yield correlated with a single high- Q^2 interaction in the Au+Au collision.

The distribution of uncorrelated background jets is determined by a mixed event (ME) procedure, in which events are mixed in exclusive bins of multiplicity, primary vertex z , and event-plane orientation. The full analysis, including jet reconstruction, is then rerun on the ME events.

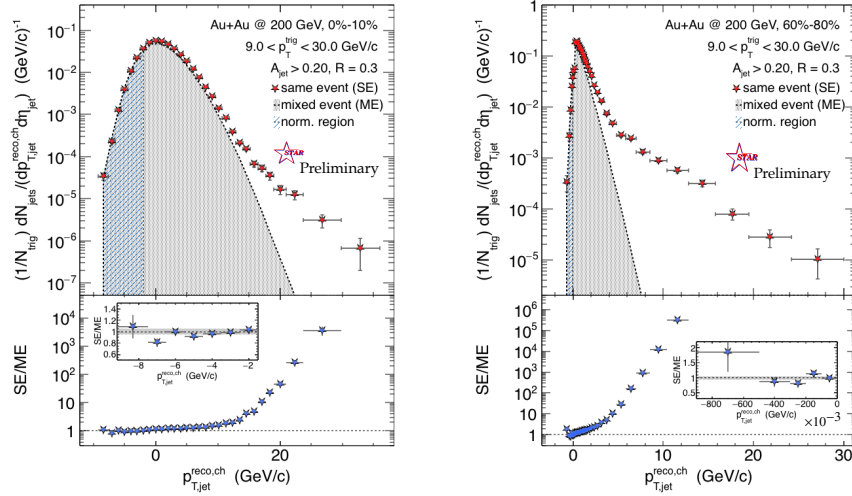


Fig. 1. Upper panels: Uncorrected recoil jet distributions for $R=0.3$ in central (left) and peripheral (right) Au+Au collisions at $\sqrt{s_{NN}}=200$ GeV, from both real (SE, red points) and ME events (shaded region). Lower panels: ratio of distributions SE/ME.

Fig. 1 shows uncorrected recoil jet distributions in real (SE) and ME events, for central and peripheral collisions. The ME jet distributions describe the real event distributions accurately for $p_{T,jet}^{reco, ch} < 0$, where uncorrelated background is expected to dominate the jet yield. At large positive $p_{T,jet}^{reco, ch}$, the SE yield is much larger than the ME yield, as expected if the correlated yield dominates. The distribution of correlated recoil jet yield is determined by subtracting the ME from the SE distribution. This raw correlated distribution is then corrected by an unfolding procedure for instrumental effects and p_T -smearing due background. The corrected recoil distributions are a function of $p_{T,jet}^{ch}$, the corrected charged-jet p_T .

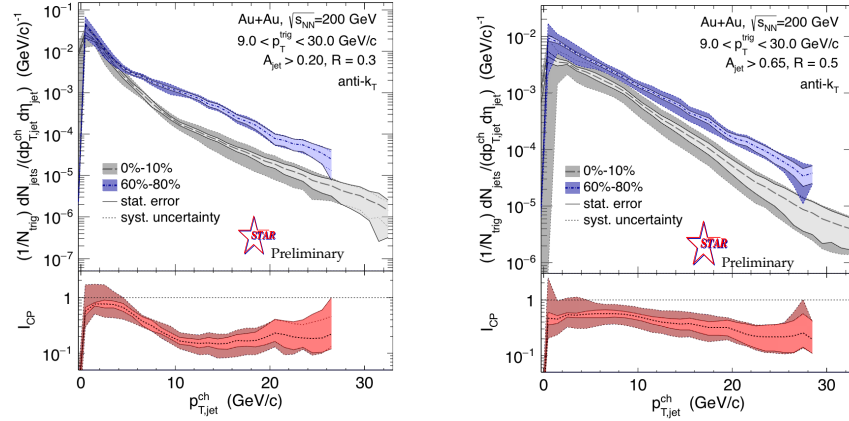


Fig. 2. Upper panels: Corrected recoil jet distributions for peripheral and central Au+Au collisions, for $R=0.3$ (left) and 0.5 (right). Lower panels: I_{CP} , the ratio of central to peripheral yield.

Figure 2, upper panels, show the corrected semi-inclusive recoil jet distributions for peripheral and central Au+Au collisions, for $R=0.3$ and 0.5 . The distributions are shown for corrected $p_{T,jet}^{ch} > 0$, with contribution from all recoil jets. The lower panels show I_{CP} , the ratio of the central to peripheral distributions. For $p_{T,jet}^{ch} > 10$ GeV/c, there is significant yield suppression in central collisions for $R=0.3$, with less suppression for $R=0.5$. In a range where the ratio is flat, the suppression in I_{CP} can be expressed equivalently as a horizontal shift between the distributions. In the range $10 < p_{T,jet}^{ch} < 20$ GeV/c, the shift is $-6.3 \pm 0.6 \pm 0.8$ GeV/c for $R=0.3$ and $-3.8 \pm 0.5 \pm 1.8$ GeV/c for $R=0.5$. ALICE has made a similar measurement for Pb+Pb collisions at $\sqrt{s_{NN}}=2.76$ TeV, finding a shift in the recoil jet distribution between pp and central Pb+Pb collisions to be -8 ± 2 GeV/c in the range $60 < p_{T,jet}^{ch} < 100$ GeV/c [1]. This shift may be interpreted as energy transport out of the jet cone due to jet quenching, in other words a direct measurement of partonic energy loss [1]. These measurements provide the first quantitative comparison of reconstructed jet quenching at RHIC and LHC.

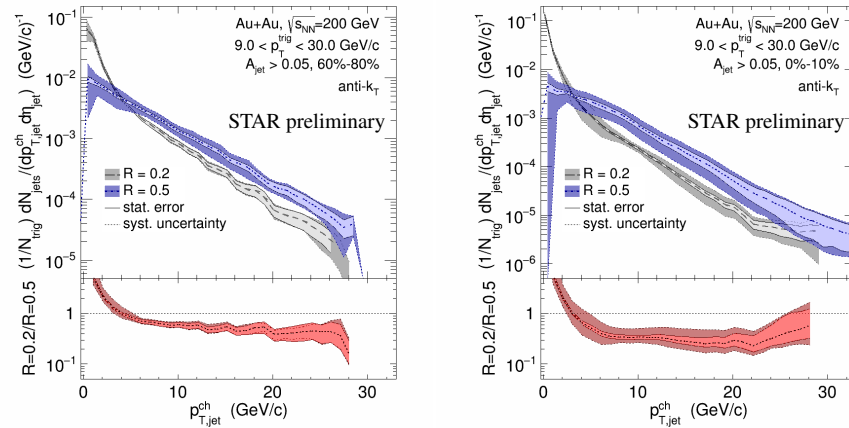


Fig. 3. Upper panels: corrected recoil distributions for $R=0.2$ and $R=0.5$, separately for peripheral (left) and central (right) Au+Au collisions. Lower panels: ratio of recoil yields for $R=0.2/R=0.5$.

For jets in pp collisions, the ratio of inclusive cross sections or semi-inclusive yields at different R

probes the distribution of intra-jet energy flow transverse to the jet axis [3, 4, 5, 1]. For jets in heavy ion collisions, such ratios provide experimentally robust observables of the modification of intra-jet structure due to quenching, [1]. Fig. 3 shows the distribution of corrected recoil jet yields for $R=0.2$ and $R=0.5$ (upper panels) and their ratio (lower panels), for peripheral and central Au+Au collisions. In the region $p_{T,\text{jet}}^{\text{ch}} > 10 \text{ GeV}/c$, the weight of the distribution is lower for central than for peripheral collisions, suggesting medium-induced intra-jet broadening within angle $R < 0.5$. However, the current uncertainty bands are also consistent with absence of medium-induced broadening in this range. A similar picture is obtained from current measurements of Pb+Pb collisions at the LHC [1].

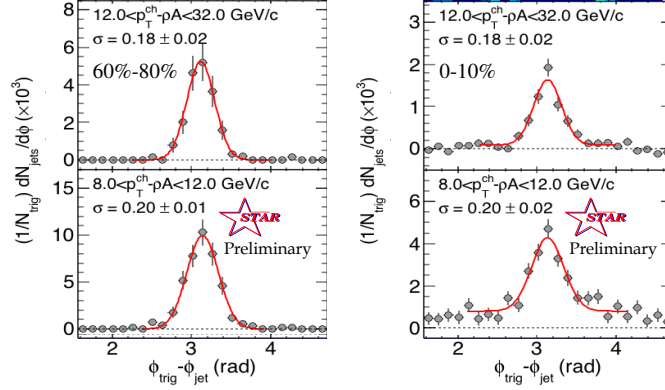


Fig. 4. Distribution of $\Delta\phi$ for two bins in uncorrected jet energy in peripheral (left) and central (right) Au+Au collisions at $\sqrt{s_{\text{NN}}}=200 \text{ GeV}$. Uncorrelated yield has been subtracted, but jet energy is not corrected for instrumental and background effects.

Acoplanarity of a di-jet pair in vacuum arises from radiation emitted at angles greater than R to the jet centroid. In heavy ion collisions, medium-induced di-jet acoplanarity may also occur [6, 7]. At sufficiently large angular deviation, hard scattering off quasi-particles in the medium (the QCD analog to Molière scattering) may dominate the angular distribution between trigger axis and recoil jet, with soft multiple scattering and radiative processes being sub-dominant [6]. Such measurements could discriminate between a medium that has discrete quasi-particles, and one that is effectively continuous at the Q^2 scale being probed [6].

Figure 4 shows the first search for QCD Molière scattering at RHIC. The $\Delta\phi$ distribution of recoil jets (Eq. 2) is shown for two bins at low jet energy in peripheral and central collisions, for jets with $R=0.3$. In this case, uncorrelated background is corrected by subtraction of the ME distribution, but the jet energy is not corrected for instrumental effects and background fluctuations.

Since the distribution is semi-inclusive, and thereby absolutely normalized, the yield in the large-angle tails relative to the trigger axis ($|\pi - \Delta\phi| > \sim 1$) can provide a direct measurement of the rate of Molière scattering. Comparison of the tails of the distributions indeed shows non-zero yield at large angles for the lower jet energy bin in central collisions, similar to the signal expected from Molière scattering. However, other effects such as flow may contribute to the signal in this region, and we do not claim evidence of Molière scattering based on this distribution. It rather serves to illustrate both the potential and the subtleties of this measurement. The fully corrected distribution, and future measurements with higher integrated luminosity, will provide constraints on the Molière scattering process.

References

- [1] J. Adam, et al., JHEP 09 (2015) 170. [arXiv:1506.03984](#).
- [2] M. Cacciari, G. P. Salam, G. Soyez, JHEP 04 (2008) 063. [arXiv:0802.1189](#).
- [3] G. Soyez, Phys.Lett. B698 (2011) 59–62. [arXiv:1101.2665](#).
- [4] B. Abelev, et al., Phys.Lett. B722 (2013) 262–272. [arXiv:1301.3475](#).
- [5] S. Chatrchyan, et al., Phys. Rev. D90 (7) (2014) 072006. [arXiv:1406.0324](#).
- [6] F. D’Eramo, M. Lekaveckas, H. Liu, K. Rajagopal, JHEP 05 (2013) 031. [arXiv:1211.1922](#).
- [7] X.-N. Wang, Y. Zhu, Phys.Rev.Lett. 111 (2013) 062301. [arXiv:1302.5874](#).